Wear and tear measurement of lathe tool using wavelets*

SHWETA KUMARI[1,2], CHARU PATHAK[3] AND SHRUTI VASHIST[4]
[1,3,4] *Department of Electronics and Communication Engineering*
Manav Rachna University, Faridabad, India
[2] *Department of Electronics and Communication Engineering, School of Engineering and Sciences*
G.D. Goenka University, Gurgaon, India

In smart manufacturing and mechanical automation, precise tool positioning is critical, particularly in the manufacturing of micro parts where accuracy at the millimeter level is essential. Thus, an attempt has been put ahead to put into place a low-cost and precise tool positioning system that can work directly with tool images that have been taken by a high-resolution camera. The goal is to calculate the positional inaccuracies of a moving lathe tool so that an auto-alignment system can get feedback. It also aims at estimating the lathe tool's dimensions, which can help with long-term wear and tear monitoring. Experimental analysis revealed that, when estimating the distances traveled by the tool from its origin using the Euclidean distance, the Sobel operator with a non-local means filter for denoising results in minimum and maximum absolute error values as 0.0011 and 0.1815, respectively. Before edge detection methods may be used, image denoising is necessary to improve their effectiveness. Because of this, the non-local means filter is particularly good at eliminating noise while keeping fine structure and features, ensuring that minute details and edges are preserved with the least amount of loss. But as noise levels rise, the non-local means filter's effectiveness declines, resulting in blurry images and a loss of clarity in the denoised output. For improved achievement, the Sobel operator with the (Daubechies) db1 wavelet at level 1 based on the findings of Stein's unbiased risk estimate (SURE) is combined. One pixel value as 0.0849 mm was achieved using level dependent SURE soft algorithm in earlier paper. Also, by applying the suggested technique for calculating the dimensionality of the lathe tool, the length of the lathe tool that is attached to the motor is 12.3105 mm, not attached to the motor is 12.2259 mm. The left side length of the lathe tool is 4.5846 mm in length, while the right side measures 4.500498 mm.

Keywords: Image Processing, Sobel, Daubechies, Lathe Tool, MATLAB

1. INTRODUCTION

Tool placement that is exact and accurate apart from dimensional measurements of cutting, milling, and lathe tools are suitable in a variety of fields, principally mechanical engineering, manufacturing, and health. Such utilization require the level of accuracy as low as the millimeter range. It is necessary to use micro-level sensors in the present-day technology to be able to accurately figure-out the dimensions and position of devices.

Using a wide range of instrument placement techniques, inclusive of coordinate measuring machines, laser interferometers, offset measurement techniques, and atomic force microscopes, has extended in the course of several years in the past. The result of this process are impacted by both static and dynamic tool location. Consequently, the most important factor in regulating contouring at fast traversal rates is dynamic data. The CNC machine makes use of error measurements in such cases, therefore setting up a position feedback system is needed. The adjustability of these measurements can improve a Machine's perceived reversal peaks, kv factor, and other attributes can be improved by adjustments of error measurements. Linear axes and rotary axes fixed positioning influences both the geometric accuracy and the thermal behavior of a machine. In this context, a framework utilizing image processing has b`een devised for a real-time positioning and dimensioning system, aimed at verifying precise tool positioning within the millimeter range. Using an image of the tool for positioning and measuring its size, brings many advantages, especially for increasing the accuracy in cutting. It was observed that both the state of the tool's wear and its orientation can ultimately shift the accuracy of the machinery.

It is desirable to place an imaging tool within millimeters of its desired position and project its wear through optimization techniques. In most of the mechanical engineering applications, such as cutting tool precision and accuracy are crucial.

The very accurate instrument represents a major step forward in the direction of more accurate micro-machine placement and measurement. Therefore, edge detection techniques are utilized initially to figure out the object edges across each image. The research focuses on overcoming specified restrictions and problems associated with traditional tool positioning methods like a coordinate measuring machine, an offset measurement technique, an atomic force microscope, or laser interferometers. The accuracy of the methods is limited by sensor drifts and noise. It also did not produce data accurate enough to use for real distance measurements, since its contact area error is large.

Limitation of sensor drifts and noise are overcome by a non-contact technique based on image processing. The proposed technique seems to be appropriate as positioning assistance throughout the different applications where precise location of the tool is important for the successful results.

2. LITERATURE REVIEW

The problem of tool positioning and verification established on the machine vision system is treated to be significant research area because of its widespread use in many industrial, aerospace, medical, and mechanical processes [1]. Earlier, there were instruments such as scanning electron microscopes, coordinate measuring machines, linear encoders, actuators, laser interferometers, atomic force microscopes, and other similar tools to measure and ensure the correctness of the tool positions [2]. An edge is beneficial for precise positioning as thresholding distinguishes and isolates a plane, an object, or a feature from other elements [3]. Because of the cutting tool's wear during machining, temperatures and tensions within the cutting zone vary constantly in robotic surgery, automated manufacturing applications, etc. [4]. As an example within the medical field, a robot was engineered explicitly for conducting eye surgery, demanding exceptionally high precision [5]. In any of these applications, tools must be replaced at specific intervals. If tools are replaced too frequently and prematurely, machine downtime will rise, leading to increased material and output costs. However, prolonging the replacement time might lead to the acquisition of low-quality or, in the worst case, the machines are completely broken down [6]. Micro-cutting technology has many benefits and they include low processing cost, flexibility, high surface finish combined with high speed and accuracy, and the ability to machine very small intricate parts. Due to the small size of tools and components in micro-machining processes, coupled with the requirement for exceptional machining accuracy, tool wear significantly affects processing quality [7]. Hence, several methods have been devised to determine the position and dimensions of tools with accuracies up to the millimeter level.

These techniques can be broadly divided into two categories: direct approaches and indirect ways. Furthermore, there are numerous of additional applications in which accurate tool dimensions and placement are crucial. The conditions of tool wear are frequently assessed indirectly through factors such as main shaft current, acoustic emission, properties of machined surfaces, and surface quality. To directly assess the degree of tool wear, direct tests often utilize machine vision or an optical microscope [8]. Image segmentation is a crucial step in computer vision, image processing, and image recognition. The extraction of the desired area relies on a set of criteria that divide an input image into several related images belonging to the same category [9]. The level of accuracy required in all the mentioned applications is at the micron scale. The contact method for measuring the travel distance of a piezoelectric motor's tool has several inherent limitations. The accuracy or error level of sensors is not assured, and the presence of flaws accelerates the rendering of data unusable due to drifts and noise. This study aims to achieve precise tool positioning at the millimeter level, with image processing selected as the method to attain this goal owing to its capability to improve accuracy.

Many researchers have delved into this research area, employing machine vision-based techniques to quantify tool wear. Lai and Fang introduced a hybrid image alignment method named the Fast Localization System utilizing the FLASH (Advanced Search Hierarchy) approach. This technique compares images to detect inconsistencies in pattern localization [10]. Niola et al. used a vision system for planning the path of the robots used in industry [11]. Nian and Tarng devised a method for a three-axis auto-alignment system utilizing vision-based inspection, which integrates the input-output system with feedback [12]. Asadpour and Golnabi explore applications and system designs for industrial machine vision [13]. Some authors have utilized methods such as the Horn-Schunck algorithm for real-time human motion detection and CMM embedded systems for movement detection [14][15][16]. Kurada et al. devised a machine vision technique to measure wear on the flanks. They utilized picture thresholding to highlight wear areas [17][18]. In numerous mechanical engineering applications, cutting tool position is a crucial factor for ensuring accuracy and precision. With the ongoing trend toward miniaturization in mechanical and optical products, there is a growing demand for exceedingly precise dimensional measurements of micro parts. Developing micro-machines necessitates precise positioning and measurement of ultra-precise equipment [19][20][21][22]. Here, in the study, image processing and segmentation approaches employing various thresholding techniques as tools for visual positioning are employed. This allows for achieving the utmost precision in tool positioning at the millimeter level. To properly place the cutting tool at the appropriate position, it is essential to accurately recognize sharp edges in images [23][24]. These methods can facilitate accurate positioning in robotic surgery, milling machines, lathe machines, and other machinery requiring precise positional accuracy [25][26][27]. Accurate measurement of micro part dimensions is critical, especially with the technological advancements enabling the miniaturization of medical products [28][29][30][31]. In milling operations, for example, the tool used to produce everyday items may experience wear over time [32][33][34]. Changes in tool dimensions diminish tool efficiency. Hence, the tool should be promptly replaced once its condition has been evaluated. Indirect tool condition monitoring using sensors such as microphones and accelerometers can incur high costs. Direct tool condition monitoring can be conducted using MATLAB software's image processing package [35][36]. Images captured by cameras undergo processing on a computer using an image processing algorithm. Even today, many computer vision systems commonly utilize Canny edge detection as a pre-processing phase. This technique is straightforward yet effective [37][38].

Numerous denoising approaches and techniques, such as those introduced by Buades et al. [39], have been proposed. Recently, they introduced a non-local means (NL means) filter, which systematically leverages all potential self-predictions within the image and the similarity of local patches to calculate pixel weights. When the patch size decreases to a single pixel, the NL means filter effectively transforms into the Bilateral Filter (BF). The former excels at preserving edges and fine structures without sacrificing too many details, whereas the latter tends to lose details and introduce irregularities along edges. Additionally, Kervrann and Boulanger [40] expanded upon the previous work by introducing adaptive control over the neighborhood of each pixel. All of these denoising methods demonstrate effectiveness in scenarios with lower noise levels (high SNR) but struggle to perform adequately when confronted with higher levels of noise (low SNR). Because both the target pixel and the similar local patches used to calculate pixel weights contain noise, the NL means filter's estimation becomes biased [41]. Addressing the issue of noisy target pixels, proposes adapting the central kernel weight (AKW) placed on the level of noise. Nevertheless, this method does not take into consideration the existence of comparable loud local patches. Consequently, particularly in cases of higher noise levels, the biased estimate exacerbates image degradation by significantly reducing image details. Therefore, over the past two decades, there has been a surge in research focusing on utilizing the wavelet transform for denoising due to its multi-resolution and energy compaction characteristics [42][43].

As indicated by the literature survey, contact methods for measuring the distance traveled by a precision DC motor-attached tool may exhibit limitations in accuracy and precision owing to sensor drifts and noise. In applications prioritizing precision and accuracy, non-contact methods for distance measurement can offer greater reliability and effectiveness.

Machine vision and image processing using MATLAB can be utilized to create a non-contact method for measuring the distance traveled by a precision DC motor-attached tool. The approach entails comparing the traveled distance to a predetermined target distance, facilitating error identification and enabling automatic alignment of the tool. Such non-contact techniques are important in the biomedical field, where small movements can have big effects.

This technology can be integrated into robotic surgical equipment and used as a positioning device, among other uses in the biomedical area [44]. Precisely and reliably measuring distances without contact can greatly enhance the precision and effectiveness of surgical tools, ultimately improving patient outcomes. Certainly, the applications of non-contact distance measurement using machine vision and image processing extend beyond the biomedical field. In smart manufacturing and mechanical automation, where precision and accuracy are paramount, non-contact methods of distance measurement can be exceptionally effective.

3. PROPOSED METHOD AND ALGORITHM

Figure 1 shows the the camera captured image [45]. Which is then acquired to a computing unit through a controller card. The tool position (2D) before and after movement in x direction is being processed.

Figure 1. Pixel positions at Lathe tool

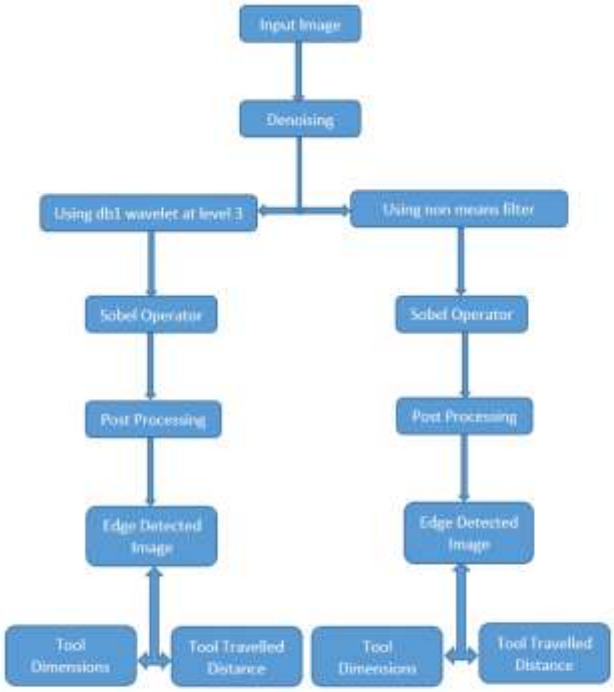

Figure 2. Flow Chart of Edge Detection, Dimensions Calculation, Travelled distance calculation

The complete process flow is presented in Figure 2. Pre-processing of the image involves converting images to grayscale images, and denoising the image using Daubechies (db1) wavelet at level 1 [46] for removing Gaussian noise. wavelet based denoising result is best for Daubechies (db1) wavelet at level 1 among other wavelets due to their capability of analysing the images at various levels keeping the sharp edge details while still trying to clean the image. Wavelet orthogonal basis is designed using the conjugate mirror filter H(ω) as shown in (1) and (2).

$$\left|H_{\emptyset}(\omega)^2 + H_{\phi}(\omega+\pi)\right|^2 = 2 \quad (1)$$

$$H_{\emptyset}(0) = \sqrt{2} \quad (2)$$

Wavelets are oscillations that have some amplitude value. They start at zero then increase, and again decrease back to 0. This looks like the brief oscillations that occur on a seismograph as shown in Figure 3.

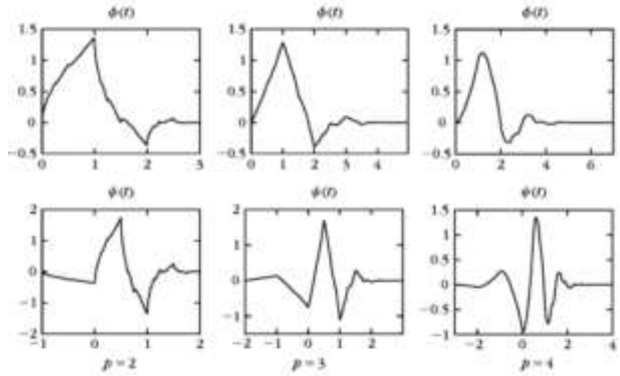

Figure 3. Representation of Daubechies Orthogonal Wavelet Family

Segmentation is performed on a Gray-scale tool image by applying a threshold value of 150 which converts it into a binary tool image. The threshold value of 150 was chosen because, upon testing with various values, this value yielded the most visually effective segmentation results. Once the tool image is segmented, the Sobel operator mask is employed to locate the coordinates for the tool edges. To ensure precise tool positioning, edge coordinates are detected along with vertices post-application of the Sobel Operator. Sobel operation over tool image matrix A defined by the matrices Gx and Gy is as given in (3).

$$Gx = [-1\ 0\ 1; -2\ 0\ 2; -1\ 0\ 1] * A; \text{ and}$$
$$Gy = [1\ 2\ 1; 0\ 0\ 0; -1 -2 -1] * A; \quad (3)$$

Where, A is the source image, Gx and Gy are the images obtained following the use of the Sobel operator. Subsequently, travelled distance are computed utilizing the Euclidean distance as specified in (4).

$$[\mathrm{sqrt}((x_2-x_1)^2+(y_2-y_1)^2)] \quad (4)$$

Where, in the provided equation, x_2 represents the pixel coordinates of the second image along the horizontal line, x_1 represents the pixel coordinates of the first image along the horizontal line, y_2 represents the pixel coordinates of the second image along the vertical line, and y_1 represents the pixel coordinates of the first image along the vertical line.

Similarly, dimensions are computed using the Euclidean distance formula directly from the pixel coordinates of each corner of the lathe tool.

Table 1. Error in travelled distance (Denoising using wavelet)

Tool Displacement (mm)	Sobel BR (movement x-axis) (mm)	Absolute Error (mm)	Relative Error
1	0.9999	-0.0001	-0.0001
2	1.9998	-0.0002	-0.0001
3	2.9997	-0.0003	-0.0001
4	3.9996	-0.0004	-0.0001
5	5.0904	0.0904	0.0181
6	6.0903	0.0903	0.0151
7	7.0902	0.0902	0.0129
8	8.1810	0.1810	0.0226
9	9.1809	0.1809	0.0201

Table 2. Error in travelled distance (Denoising using Non Means Filter)

Tool Displacement (mm)	Sobel BR (movement x-axis) (mm)	Absolute Error (mm)	Relative Error
1	1.0040	0.0040	0.0040
2	2.0019	0.0019	0.0009
3	3.0011	0.0011	0.0003
4	4.0915	0.0915	0.0228
5	5.0912	0.0912	0.0182
6	6.0910	0.0910	0.0151
7	7.0908	0.0908	0.0129
8	8.1815	0.1815	0.0226
9	9.1813	0.1813	0.0201

4. EXPERIMENTAL SETUP AND RESULTS

To conduct experiments and test the proposed algorithms, the experimental setup included imaging capabilities like PC, Piezoelectric motor, Motion card, CCD camera, Vibration isolation table, MATLAB software, IEEE 1394b FireWire Controller Card. The experimental setup also included a moving Lathe tool and a stationary work piece. It facilitates image capture of the lathe tool at various positions, with increments of 1 mm. The Lathe tool is displaced in the X direction. The methodology encompasses calibrating the imaging system of the setup using a standard calibration grid, determining a pixel value of 0.0849 mm [47]. It has been found that level dependent SURE soft algorithm results into best SNR and least value of MSE. Based on this observation, one pixel value in real world was determined. In all the positions, vertex c coordinates of the Lathe tool are obtained as shown in Figure 1. Edge methods for detection are being used to get these coordinates. Euclidian distance traveled from the starting point of the tool are calculted. Analysis was done for the movement of 1 to 9 mm. Here, in Table 1, an inaccuracy of millimeters when calculating small distances traveled by the tool is a compelling error. The absolute error is sufficient since it provides information about the error's significance. As stated in (5), absolute error is the discrepancy between tool movement based on images and actual tool movement.

$$\Delta x = x_0 - x \quad (5)$$

Where, x_0 represents the image-based tool movement, and x represents the actual tool movement, and Δx is referred to as an absolute error. The range is -0.004 to 0.1810.

The relative error indicates the extent of the error in relation to the correct value, whereas the absolute error indicates how far us the error overall. (6) defines the relative error as the proportion of the measurement's absolute inaccuracy to the tool's actual movement.

$$\mathrm{RelativeError} = (x_0 - x)/x = \Delta x/x \quad (6)$$

In this instance, the image-based movement is represented by x_0, the actual movement by x, and the absolute inaccuracy by Δx. MAE is the average absolute error between actual and image-based values as mentioned in (7).

$$MAE = \frac{1}{n}\sum_{i=1}^{n}|x_i - x| \tag{7}$$

Where, $|x_i - x|$ is absolute errors and, the number of errors is n. The closer MAE is to 0, the more accurate the algorithmic model is. Here, algorithmic model accuracy is 0.0702.

(8) illustrates how to utilize variance to get the expected difference in deviations from the actual value.

$$\mathrm{Var}(X)=[(x_1-\bar{x})^2+(x_2-\bar{x})^2+(x_3-\bar{x})^2+\ldots\ldots+(x_n-\bar{x})^2]/n \tag{8}$$

Where, values are x_1, x_2, x_3, x_4,... n. The average value is $\bar{x}$. The variance of 7.0138 is observed here and the deviation observed is 2.648358 and is a measure of how spread out the image-based values is.

Similarly, in Table II, where an error in the traveled distance is calculated by using a non-means filter during the denoising process, the absolute error in the measured distance lies in the range of 0.0011 and 0.1815.

In the proposed method appears to perform slightly better, especially at smaller displacements (1-4 mm), their improvements are marginal at larger displacements due to non-uniform illumination of light from below.

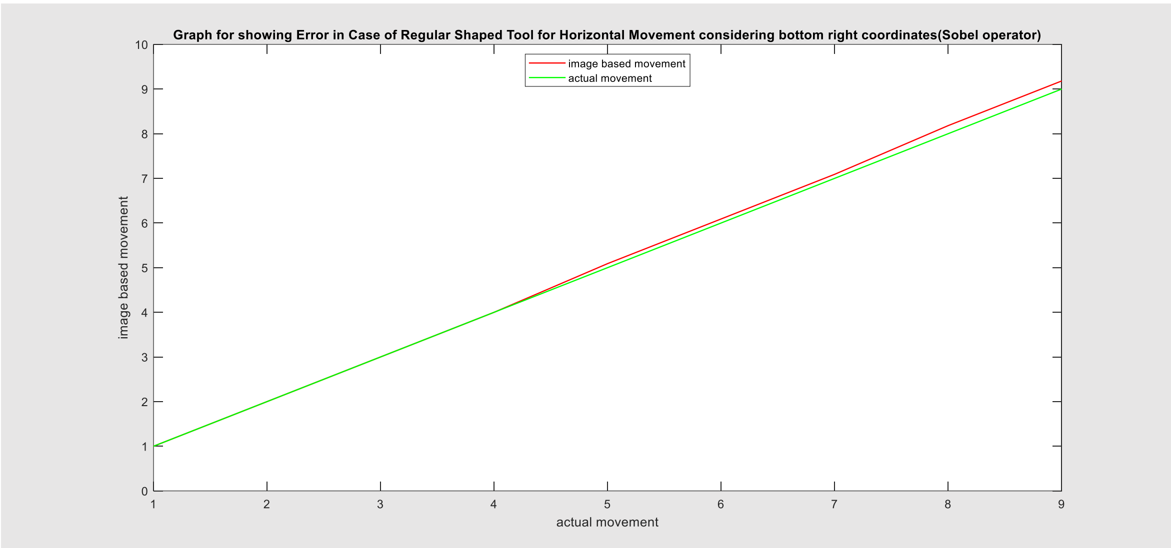

Figure 4. Graph showing the error in case of horizontal movement (Denoising using Wavelet)

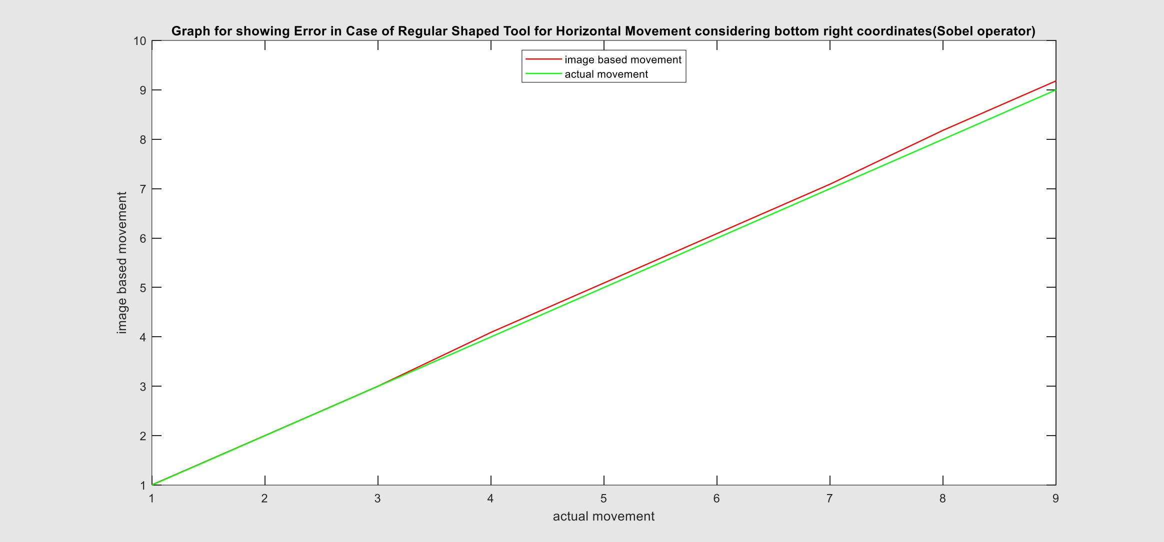

Figure 5. Graph showing the error in case of horizontal movement (Denoising using Non Means Filter)

Figure 4 and Figure 5 show the graphs for absolute error in millimeters range for the tool moved at a distance of 1mm. The tool is moved in X directions. The positions of the tool are estimated by estimation of the position of the bottom right (BR) vertex of the tool at a time respectively.

Observation reveals very small error value when denoising is performed using Sobel operator along with wavelet which is almost close nearly zero in comparison to the denoising performed using non-means filter, which is additionally around 0.090 millimeters.

Figure 6 shows the output images at different stages of edge detection. It shows the noisy, denoised, filtered, edge detected and colored edge detected image for before and after movement of 9 mm when db1 wavelet denoising along with the Sobel operator is applied.

When millimeter accuracy is required, the Sobel operator performs better and provides more accurate results when pre-processed with Daubechies wavelets for denoising.

Figure 1 displays the pixel positions at each corner of the lathe tool. Consequently, the pixel coordinates of the vertex of the lathe tool are calculated as displayed in Table 3.

Table 3. Pixel Coordinates of LatheTool

Vertex of Lathe tool	Pixel Coordinate (x, y)
a	(1, 885)
b	(1, 1030)
c	(54, 1029)
d	(55, 885)

The lathe tool is positioned horizontally, with the edges attached to the motor having corners labeled as a and b, and the edges away from the motor having corners labeled as c and d. Each corner (a, b, c, and d) has specific coordinates (x, y). The lathe tool moves either in the x direction or the y direction. The dimensions of the lathe tool in its original position are being calculated as demonstrated in Table 4. For all calculation purposes one pixel value is held as 0.0849 mm, which was achieved earlier after camera calibration. Using Equation (4), the length of the section ab attached to the motor between coordinates (1,885) and (1, 1030) comes out to be 145 pixels and is converted to real-world as 12.3105 mm based on one pixel value as 0.0849. The length of the section cd between coordinates (54, 1029) and (55, 885) which is away from the motor is 4.500498mm. The left side length bc measures 4.500498 mm between (1, 1030) and (54, 1029), and the right side length da is 4.5846mm between coordinates (55,885) and (1,885). These calculated lengths are crucial for detecting wear and tear of the lathe tool over longer period of time.

Table 4. Pixel Coordinates of LatheTool

Vertex of Lathe tool	Euclidean Distance (pixels) between Vertex of Lathe Tool	Euclidean Distance (mm) between Vertex of Lathe Tool
Length ab	145.0000	12.3105

Length bc	054.0000	04.5846
Length cd	144.0035	12.2259
Length da	053.0094	04.5004

In Table 4, hence, it is noticed that the length of ab of the lathe tool is greater in length than length of cd. Additionally, length of bc is greater in length than length of da of the lathe tool. Therefore, the lathe tool has a trapezoidal shape.

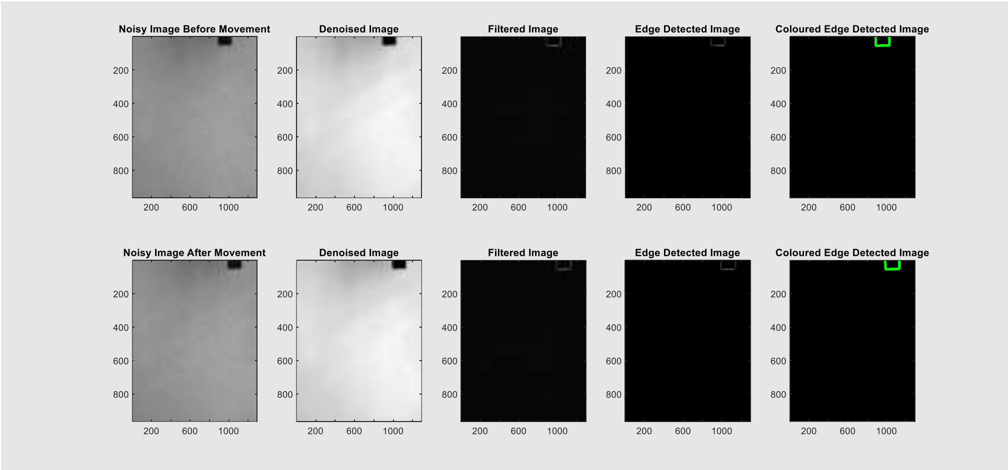

Figure 6. Edge detection for X-axis movement of Lathe tool considering (Bottom Right) BR coordinates (Sobel operator)

5. CONCLUSION

Provide A merger of db1 wavelet established on the SURE denoising method with the Sobel operator gives an improvement in minimum and maximum absolute error values as -0.0004 and 0.1810 respectively. Hence, the Sobel operator succeeds better and generates more accurate results when preprocessed using Daubechies wavelets when a preciseness of mm needed for denoising. Compared to other operators, the Sobel operator computes quickly, which facilitates the finding of clean edges. Furthermore, because the coefficient's magnitude does not exist, a higher weight can be imposed to the mask, results in sharper edges and superior edge visibility.

The SURE denoising technique efficiently eliminates enough Gaussian noise to reconstruct the details of an image when the Daubechies wavelet at level 1 is employed.

In the industrial, healthcare, and other fields, automation has contributed to a growing demand for highly precise technology. As a result of the present study, more precise robotic devices that can recognize and alert users to differences in the positioning and dimensions of lathe tools will be designed. These technologies would be image-based, low-cost, and contactless.

REFERENCES

1. E. N. Malamas, E. G. M. Petrakis, M. Zervakis, L. Petit, and J.-D. Legat, "A survey on industrial vision systems, applications and tools," Image and Vision Computing, vol. 21, no. 2, pp. 171–188, Feb. 2003, doi: https://doi.org/10.1016/s0262-8856(02)00152-x.
2. E. Ribeiro and M. Shah, "Computer Vision for Nanoscale Imaging," Machine Vision and Applications, vol. 17, no. 3, pp. 147 162, Jun. 2006, doi: https://doi.org/10.1007/s00138-006-0021-7.
3. D. Apostol, V. Damian, And P. C. Logofatu, "Nanometrology of microsystems: Interferometry," Romanian Reports in Physics, vol.60,no.3,Jan.2008,Available:https://www.researchgate.net/publication/241188714_Nanometrology_of_microsystems_Interferometry.
4. D. Vikram Mutneja, "Methods of Image Edge Detection: A Review," Journal of Electrical & Electronic Systems, vol. 04, no. 02, 2015, doi: https://doi.org/10.4172/2332-0796.1000150.
5. T. Bergs, C. Holst, P. Gupta, and T. Augspurger, "Digital image processing with deep learning for automated cutting tool wear detection," Procedia Manufacturing, vol. 48, pp. 947–958, 2020, doi: https://doi.org/10.1016/j.promfg.2020.05.134.
6. T. Tayama et al., "Image Processing for Autonomous Positioning of Eye Surgery Robot in Micro-Cannulation," Procedia CIRP, vol. 65, pp. 105–109, Jul. 2017, doi: https://doi.org/10.1016/j.procir.2017.04.036.

7. T. Xi, I. M. Benincá, S. Kehne, M. Fey, and C. Brecher, "Tool wear monitoring in roughing and finishing processes based on machine internal data," The International Journal of Advanced Manufacturing Technology, vol. 113, no. 11–12, pp. 3543–3554, Mar. 2021, doi: https://doi.org/10.1007/s00170-021-06748-6.

8. Z. Yu, L. Zhang, K. Xia, L. Zhang, and H. Yu, "Tool wear inspection method for small lathe," 2014 IEEE International Conference on Mechatronics and Automation, pp. 1161–1165, Aug. 2014, doi: https://doi.org/10.1109/icma.2014.6885862.

9. I. N. Tansel et al., "Tool wear estimation in micro-machining.," International Journal of Machine Tools and Manufacture, vol. 40, no. 4, pp. 599–608, Mar. 2000, doi: https://doi.org/10.1016/s0890-6955(99)00073-5.

10. Jeevitha Kuppan, "A Review On Various Segmentation Techniques In Image Processsing," European Journal of Translational and Clinical Medicine, vol. 7, no. 4, pp. 1342–1348, Nov. 2020, Available: https://www.researchgate.net/publication/357647988_A_Review_on_Various_Segmentation_Techniques_in_Image_Processsing.

11. V. Niola, C. Rossi, and S. Savino, "An Application of Vision Systems to the Path Planning of Industrial Robots," Lecture Notes In Computer Science, pp. 586–594, doi: https://doi.org/10.1007/978-3-540-75555-5_56.

12. H. T. Kim, C. S. Song, and H. J. Yang, "2-Step algorithm for automatic alignment in wafer dicing process," Microelectronics Reliability, vol. 44, no. 7, pp. 1165–1179, Jul. 2004, doi: https://doi.org/10.1016/j.microrel.2004.01.005.

13. H. Golnabi and A. Asadpour, "Design and application of industrial machine vision systems," Robotics and Computer-Integrated Manufacturing, vol. 23, no. 6, pp. 630–637, Dec. 2007, doi: https://doi.org/10.1016/j.rcim.2007.02.005.

14. C.Y. Nian and Y.S. Tarng, "An auto-alignment vision system with three-axis motion control mechanism," The International Journal of Advanced Manufacturing Technology, vol. 26, no. 9, pp. 1121–1131, Oct. 2005, doi: https://doi.org/10.1007/s00170-004-2079-6.

15. Jaiganes a/l Kanawathi, Siti Salasiah Mokri, N. Ibrahim, A. Hussain, and M. M. Mustafa, "Motion detection using Horn Schunck algorithm and implementation," International Conference on Electrical Engineering and Informatics, Aug. 2009, doi: https://doi.org/10.1109/iceei.2009.5254812.

16. P. Mahapatra, S. Ganguli, and A. Kumar, "A hybrid particle swarm optimization and artificial immune system algorithm for image enhancement," Soft Computing, vol. 19, no. 8, pp. 1–9, Jul. 2014, doi: https://doi.org/10.1007/s00500-014-1394-6.

17. R. J. Hocken and P. H. Pereira, Eds., Coordinate Measuring Machines and Systems. CRC Press, 2016. doi: https://doi.org/10.1201/b11022.

18. P. M. P, "Tool Wear Monitoring By Image Processing," vol. 8, no. 2, pp. 2731–2738, Aug. 2013, Available: https://www.researchgate.net/publication/332763470_Tool_Wear_Monitoring_By_Image_Processing.

19. S. Kurada and C. Bradley, "A review of machine vision sensors for tool condition monitoring," Computers in Industry, vol. 34, no. 1, pp. 55–72, Oct. 1997, doi: https://doi.org/10.1016/s0166-3615(96)00075-9.

20. E. Sharma, None Shivali, None Jyotsna, P. Mahapatra, and Amit Doegar, "Tool condition monitoring using the chain code technique, pixel matching and morphological operations," pp. 1–6, Feb. 2017, doi: https://doi.org/10.1109/ciact.2017.7977270.

21. L. Maurya, V. Lohchab, P. Kumar Mahapatra, and J. Abonyi, "Contrast and brightness balance in image enhancement using Cuckoo Search-optimized image fusion," Journal of King Saud University - Computer and Information Sciences, vol. 34, no. 9, pp. 7247–7258, Oct. 2022, doi: https://doi.org/10.1016/j.jksuci.2021.07.008.

22. P. K. Mahapatra, Spardha, I. K. Aulakh, A. Kumar, and S. Devi, "Particle Swarm Optimization (PSO) based Tool Position Error Optimization," International Journal of Computer Applications, vol. 72, no. 23, pp. 25–32, Jun. 2013, Accessed: Jan. 29, 2025. [Online]. Available: https://www.ijcaonline.org/archives/volume72/number23/12683-9461/

23. P. K. Mahapatra, A. Garg, and A. Kumar, "Error Optimization of Machine Vision based Tool Movement using a Hybrid CLONALG and PSO Algorithm," International Journal of Applied Metaheuristic Computing, vol. 7, no. 1, pp. 65–78, Jan. 2016, doi: https://doi.org/10.4018/ijamc.2016010104.

24. E. Ribeiro and M. Shah, "Computer Vision for Nanoscale Imaging," Machine Vision and Applications, vol. 17, no. 3, pp. 147–162, Jun. 2006, doi: https://doi.org/10.1007/s00138-006-0021-7.

25. Sagrario Lantarón, Mariló López, and Javier Rodrigo Hitos, "A Doubly Adaptive Algorithm for Edge Detection in 3D Images," Mathematical Problems in Engineering, vol. 2016, pp. 1–16, Jan. 2016, doi: https://doi.org/10.1155/2016/4904279.

26. Sagrario Lantarón, Mariló López, and Javier Rodrigo Hitos, "A Doubly Adaptive Algorithm for Edge Detection in 3D Images," Mathematical Problems in Engineering, vol. 2016, pp. 1–16, Jan. 2016, doi: https://doi.org/10.1155/2016/4904279.

27. B. H. Yoshimi and P. K. Allen, "Visual control of grasping and manipulation tasks," Columbia Academic Commons (Columbia University), pp. 575–582, Dec. 2002, doi: https://doi.org/10.1109/mfi.1994.398402.

28. A. G. Rehorn, J. Jiang, and P. E. Orban, "State-of-the-art methods and results in tool condition monitoring: a review," The International Journal of Advanced Manufacturing Technology, vol. 26, no. 7–8, pp. 693–710, Oct. 2005, doi: https://doi.org/10.1007/s00170-004-2038-2.

29. W. Wang, "Size and Shape Measure of Particles by Image Analysis," Lecture notes in computer science, pp. 253–262, Jan. 2006, doi: https://doi.org/10.1007/11774938_20.

30. . Vega, W. Lasso, and C. Torres, "Image processing applied to measurement of particle size," Journal of Physics Conference Series, vol. 582, no. 1, pp. 012061–012061, Jan. 2015, doi: https://doi.org/10.1088/1742-6596/582/1/012061.

31. C. Shanthi, R. Kingsley Porpatham, and N. Pappa, "Image Analysis for Particle Size Distribution," International Journal of Engineering and Technology, vol. 6, no. 3, pp. 1340–1345, Dec. 2014, Available: https://www.researchgate.net/publication/287319918_Image_Analysis_for_Particle_Size_Distribution

32. T. Andersson, "Estimating particle size distributions based on machine vision," DIVA, 2016. https://www.diva-portal.org/smash/record.jsf?pid=diva2%3A991638&dswid=7328 (accessed Jan. 29, 2025).

33. J. H. Arévalo-Ruedas, E. Espinel-Blanco, and E. Florez-Solano, "Wear analysis in cutting tools by the technique of image processing with the application of two-dimensional matrices," Journal of Physics: Conference Series, vol. 2139, no. 1, p. 012018, Dec. 2021, doi: https://doi.org/10.1088/1742-6596/2139/1/012018.

34. J. A. Ghani, M. Rizal, M. Z. Nuawi, M. J. Ghazali, and C. H. C. Haron, "Monitoring online cutting tool wear using low-cost technique and user-friendly GUI," Wear, vol. 271, no. 9, pp. 2619–2624, Jul. 2011, doi: https://doi.org/10.1016/j.wear.2011.01.038.

35. P. M. P, “Tool Wear Monitoring By Image Processing,” vol. 8, no. 2, pp. 2731–2738, Aug. 2013, Available: https://www.researchgate.net/publication/332763470_Tool_Wear_Monitoring_By_Image_Processing

36. Mouloud Ourak, T. Brahim, O. Lehmann, and N. Andreff, “Direct Visual Servoing Using Wavelet Coefficients,” IEEE/ASME Transactions on Mechatronics, pp. 1–11, Feb. 2019, doi: https://doi.org/10.1109/TMECH.2019.2898509.

37. A. Rana and C. Pathak, “Wavelet Thresholding Algorithms for Image Denoising,” Indian Journal of Science and Technology, vol. 11, no. 27, pp. 1–6, Jul. 2018, doi: https://doi.org/10.17485/ijst/2018/v11i27/130706.

38. S. Naidu, A. Quadros, Arsha Natekar, Prajakta Parvatkar, and Shailendra Aswale, “Medical Image Enhancement based on Statistical and Image Processing Techniques,” vol. 10, no. 5, pp. 509–515, May 2021, Available: https://www.researchgate.net/publication/351993603_Medical_Image_Enhancement_based_on_Statistical_and_Image_Processing_Techniques.

39. J. Wedekind, “Efficient Implementations of Machine Vision Algorithms using a Dynamically Typed Programming Language,” Jan. 01, 2012. https://www.researchgate.net/publication/233986718_Efficient_Implementations_of_Machine_Vision_Algorithms_using_a_Dynamically_Typed_Programming_Language.

40. A. Buades, B. Coll, and J.-M. Morel, “Neighborhood filters and PDE’s,” Numerische Mathematik, vol. 105, no. 1, pp. 1–34, Sep. 2006, doi: https://doi.org/10.1007/s00211-006-0029-y.

41. C. Kervrann and J. Boulanger, “Optimal Spatial Adaptation for Patch-Based Image Denoising,” vol. 15, no. 10, pp. 2866–2878, Oct. 2006, doi: https://doi.org/10.1109/tip.2006.877529.

42. N. H. Xu, N. J. Xu, and N. F. Wu, “On the biased estimation of nonlocal means filter,” pp. 1149–1152, Jun. 2008, doi: https://doi.org/10.1109/icme.2008.4607643.

43. I. Daubechies, “Ten Lectures on Wavelets - Ingrid Daubechies (1992).pdf,” Google Docs, 2019. https://docs.google.com/file/d/0Bzl8fDcnItY2ZmMzlhYjUtOGZjMC00OTNiLWI0YTctNjE3OGI1M2U3OTA5/edit?resourcekey=01b3bAzqq9If928_XtEvMag (accessed Jan. 29, 2025).

44. “A Wavelet Tour of Signal Processing,” Elsevier Shop, 2024. https://shop.elsevier.com/books/a-wavelet-tour-of-signal-processing/mallat/978-0-12-374370-1

45. P. K. Mahapatra, R. Thareja, M. Kaur, and A. Kumar, “A Machine Vision System for Tool Positioning and Its Verification,” Measurement and Control, vol. 48, no. 8, pp. 249–260, Oct. 2015, doi: https://doi.org/10.1177/0020294015602499.

46. S. Kumari, C. Pathak, and S. Vashist, “Enhanced lathe tool positioning through wavelet-based image denoising techniques,” IET Conference Proceedings, vol. 2024, no. 30, pp. 321–331, Mar. 2025, doi: https://doi.org/10.1049/icp.2025.0274.

47. S. Kumari, C. Pathak, S. Vashist, and J. Singh, “Wavelet methods for noise reduction in the calibration of a CCD camera,” AIP Conference Proceedings, vol. 3227, p. 050001, 2025, doi: https://doi.org/10.1063/5.0241669.